Wavelet Correlation of Non-stationary Bursts of EEG

S. V. Bozhokin[a] and I. B. Suslova[b]
Peter the Great Saint-Petersburg Polytechnic University, Polytechnicheskaya str. 29, Saint-Petersburg, Russia

Keywords: EEG, Continuous Wavelet Transform, Wavelet Correlation Function.

Abstract: The problem of non-stationary correlation of signals recorded in various EEG channels of the human brain is considered. Each signal is represented as a sequence of bursts occurring at different times in different spectral ranges. To solve the problem of detecting the relationship of these signals, the authors introduced a new wavelet correlation function WCF. The WCF function allows you to detect the correlation of individual bursts of different EEG channels that have the same frequency, but different times of occurrence. The WCF function is built on the basis of continuous wavelet transforms of two signals taken at different points in time. For the considered recording data of two EEG channels, the burst correlations were classified. The proposed solution to the problem of correlation of EEG signals makes it possible to trace the propagation of disturbances in the cerebral cortex (traveling waves) and to reveal the synchronization of movement of evoked potentials.

1 INTRODUCTION

It is known that human electroencephalogram (EEG) shows electrical activity of a great number of neurons in the brain. The signal from each EEG channel is an alternation of bursts in different spectral ranges $\mu = \{\delta, \theta, \alpha, \beta\}$. EEG is essentially a nonstationary process, since its spectral and statistical properties change over time (Mandel and Wolf, 1995; Papandreou-Suppappola, 2003; Adeli and Ghost-Dastidar, 2010; Hramov et al., 2015). The unsteady character of EEG signal can be observed both at rest of the subject and during functional tests (photo-stimulation, hyperventilation).

To analyze changes in the spectral composition of nonstationary signals (NSs), the windowed Fourier transform (STFT - Short Time Fourier Transform) is often used (Subha et al., 2010). In this case, the entire measurement interval T is divided into a number of consecutive windows, each having the duration equal to $W = T / N$, where N is the total number of windows. The consistent behavior of two different processes $Z_J(t)$ and $Z_K(t)$ recorded from different EEG channels J and K is characterized by the value of coherence. The coherence of the brain shows the degree of intra-cortical interactions in different parts of the brain and the presence of functional relations between them.

The calculation of the coherence function includes the averaging of Fourier components of two signals over many realizations (Kulaichev, 2011; Sheikhani and Behnam, 2008; Seleznov et al., 2019; Reiser et al., 2012; Kropotov, 2012; Bendat and Pierrsol, 2011). Phase coherence of the two signals is characterized by the value $PLV_{JK}(f)$ called the Phase Locking Value (Piqueira, 2011; Trofimov et al., 2015; Duc et al. 2019). However, we should note that as shown in (Kulaichev, 2011), the value of the coherence of two signals depends on the averaging procedure, choice of the window size, window function, and the value of the window step shift.

Therefore, the coherence value cannot be considered as a strict quantitative measure of the correlation of two signals $Z_J(t)$ and $Z_K(t)$, where J and K are the numbers of EEG channels. In addition, various computer programs use different types of windows and numbers of averaging. Thus,

[a] https://orcid.org/0000-0001-5653-6574
[b] https://orcid.org/0000-0002-4497-1867

Bozhokin, S. and Suslova, I.
Wavelet Correlation of Non-stationary Bursts of EEG.
DOI: 10.5220/0010196701420149
In *Proceedings of the 14th International Joint Conference on Biomedical Engineering Systems and Technologies (BIOSTEC 2021) - Volume 4: BIOSIGNALS*, pages 142-149
ISBN: 978-989-758-490-9

it is difficult to compare the results obtained in the works of various authors.

The purpose of this work is to find the correlation of nonstationary signals from different EEG channels. We introduce the new type of correlation function, and use it to determine the matching of various EEG bursts occurring in different spectral ranges at different points in time.

2 WAVELET CORRELATION FUNCTION

Currently, the continuous wavelet transform (CWT) method is often used to quantitatively describe the nonstationary EEG (Mallat, 2008; Cohen, 2003; Advances in Wavelet, 2012; Chui and Jiang, 2013; Addison, 2017; Hramov, 2015; Bozhokin and Suvorov, 2008; Bozhokin and Suslova, 2014, 2015; Wavelets in Physics, 2004).

We determine continuous wavelet transform $V(\nu,t)$ for the time-dependent signal $Z(t)$ by the formula

$$V(\nu,t)=\nu\int_{-\infty}^{\infty}Z(t')\Psi^{*}\left(\nu(t'-t)\right)dt'. \quad (1)$$

The function $\Psi(x)$ is a mother wavelet. The * sign means complex conjugation. The mother wavelet in (1) has two properties. The average value of $\Psi(x)$ over the entire argument $-\infty<x<\infty$ is zero. The squared norm $\|\Psi(x)\|^2$ is equal to one. The main types of mother wavelets are given in the book (Hramov, 2015). In our study we use the Morlet mother wavelet function $\Psi(x)$ with the control parameter m:

$$\Psi(x)=D_m\exp\left(-\frac{x^2}{2m^2}\right)\left[\exp(2\pi ix)-\exp\left(-\Omega_m^2\right)\right], \quad (2)$$

where $\Omega_m=m\pi\sqrt{2}$. The control parameter m allows us to change the spectral and temporal resolution of the signal under study. The Fourier component $\hat{\Psi}(F)$ of the mother wavelet function and the normalization constant D_m (2) are given in (Bozhokin et al. 2017). We derive the formula

$$V(\nu,t)=\int_{-\infty}^{\infty}\hat{Z}(f)\hat{\Psi}^{*}\left(\frac{f}{\nu}\right)\exp(2\pi ift)\,df \quad (3)$$

by performing twice the Fourier transform of (1). Here $\hat{Z}(f)$ is the Fourier component of the signal $Z(t)$.

Consider the particular case of an infinite harmonic signal $Z(t)=\cos(2\pi f_0 t)$ with constant frequency f_0. The Fourier component of such a signal is the superposition of two Dirac delta functions: $\hat{Z}(f)=\left[\delta(f+f_0)+\delta(f-f_0)\right]/2$. The maximum value of $|V(\nu,t)|$ (1) will be observed exactly at the frequency value $\nu=f_0$. For $\exp\left(-2\Omega_m^2\right)<<1$, this maximum will not depend on time.

Assume that $V_J(\nu,t)$ corresponds to $Z_J(t)$ and $V_K(\nu,t)$, – to $Z_K(t)$. The cross wavelet spectrum of two signals is determined by the formula

$$CWS_{JK}(\nu,t)=V_J(\nu,t)V_K^{*}(\nu,t). \quad (4)$$

By averaging the function $CWS_{JK}(\nu,t)$ both over frequencies ν and time t, and by normalizing this value, one can obtain the square of the wavelet coherence function $\Gamma^2(\nu,t)$. The details of the averaging procedure for calculating the function $\Gamma^2(\nu,t)$, as well as its application to various non-stationary signals, can be found in (Lachaux et al., 2002; Klein et al., 2006; Banfi et al., 2012; Grinsted et al., 2004; Li et al., 2007; Kang et al., 2019; Chaves and Cazelles, 2019; Yang et al., 2019; Schuck and Bodmann, 2019).

Unfortunately, the values of $\Gamma^2(\nu,t)$ depend on the mother wavelet, as well as on the averaging procedure over ν and t. It is important to emphasize that the time-averaging procedure of the wavelet coherence function associated with the idea of the short time Fourier transform (STFT) negates the main advantage of CWT for studying NS, whose spectral and temporal properties can vary significantly over time. Indeed, the correlations of NS signals can develop and disappear at small time scales. However, the function $\Gamma^2(\nu,t)$ based on the averaging procedure over many epochs cannot detect this effect.

Let us introduce the wavelet correlation function $WCF_{JK}(\nu,t)$ for two signals $Z_J(t)$ and $Z_K(t)$ as

$$WCF_{JK}(v,t)=\int_{-\infty}^{\infty} V_J^*(v,t')V_K(v,t+t')\,dt'. \quad (5)$$

In contrast $CWS_{JK}(\nu,t)$ (4), the function $WCF_{JK}(\nu,t)$ (5), describes the correlation between two signals at different times. The complex conjugate wavelet transform of the first signal $V_J^*(\nu,t')$ is taken at the time moment t'. The wavelet transform of the second signal $V_K(\nu,t+t')$ is taken at time $t+t'$. Representing (5) in terms of Fourier components, we get:

$$WCF_{JK}(v,t)=\int_{-\infty}^{\infty} \hat{Z}_J^*(f)\hat{Z}_K(f)\left|\hat{\Psi}\left(\frac{f}{v}\right)\right|^2 \exp(2\pi ift)\,df. \quad (6)$$

Using the wavelet correlation function $WCF_{JK}(\nu,t)$ (5)-(6), we get an opportunity to study the correlation in time of various channels in the EEG record. The EEG signal from each channel will be a sequence of bursts occurring at different points in time in different spectral ranges $\mu=(\delta,\theta,\alpha,\beta,\gamma)$.

3 RESULTS

In this study, we use a spontaneous EEG of a healthy subject at rest with his eyes closed. The background of the EEG signal represents desynchronized activity of the neural ensembles of the cerebral cortex. In addition to the background activity, the EEG signal includes various oscillatory patterns. Such patterns represent continuously appearing and disappearing bursts of rhythms related to the coherent electrical activity of neural ensembles. When registering EEG, standard channels are used according to the 10-20% scheme, where index J =1,2, ... 21 takes the values {Fp1, Fpz, Fp2; F7, F3, Fz, F4, F8; T3, C3, Cz, C4, T4; T5, P3, Pz, P4, T6; O1, Oz, O2}. The shifts of the electrical activity maxima for different channels are small, therefore the signal sampling frequency is F_d = 500 Hz, which corresponds to the signal sampling time 2 ms.

By the burst of EEG activity in the frequency range $\mu=\{\delta,\theta,\alpha,\beta\}$, we mean appearance and disappearance of a group of waves different from the background EEG activity in frequency, shape and amplitude. The maximum electrical activity of such a burst is localized at a certain point in time $t_{\max}$. Each burst has its beginning and end, as well as its own characteristic duration. For each burst, it is possible to estimate the characteristic spectral range.

Fig.1 shows the signal $Z_J(t)$ from occipital channel O_Z.

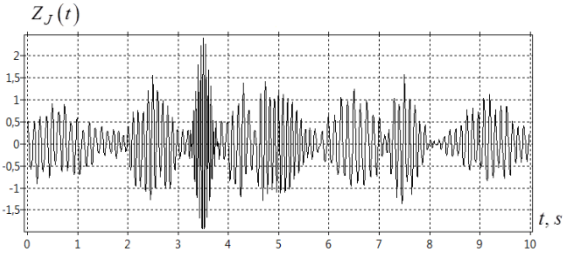

Figure 1: EEG signal time dependence (channel $J=O_Z$).

Visual analysis of $Z_J(t)$ shows the presence of alpha activity bursts ($\alpha=[7-14\ Hz]$) in the rhythm. The centers of these bursts are localized at the moments of time approximately equal to $t_J=\{0.5;$ 2.5; 4.3; 5.0; 6.5; 7.6; 9.2 s$\}$. Let us analyze the characteristic frequencies of all flashes in the $\alpha=[7-14\ Hz]$ and β [14-30 Hz] ranges using the STFT method with the window $W=2$ s. For each burst, the STFT estimation gives a characteristic burst maximum t_J, measured in s, and one or several characteristic frequencies ν_J in Hz. For signal $Z_J(t)$, we have the burst matrix $\alpha MatrixZ_J\{\nu_J;t_J\}=$ {{8.2; 0.51}, {12.0; 0.49}, {10.2; 2.58}, {13.0; 2.59}, {9.2; 4.28}, {14.0; 4.30}, {11.2; 5.10}, {7.8 ; 6.41}, {9.8; 7.62}, {8.8; 9.23}, {6.2; 9.21}}.

In addition to the natural signal $Z_J(t)$, we insert into the signal the artificial (model) burst of activity having a Gaussian shape located at $t_0=0.35$ s. This burst has constant frequency $\nu_0=20$ Hz and characteristic half-width $\tau_0=0.09$ s. In β -range, the total matrix of signal bursts $Z_J(t)$ has the form $\beta MatrixZ_J\{\nu_J;t_J\}=$ {{20.0; 3.50}, {15.1; 5.18}, {16.3; 6.11}, {16.9; 7.43}, {18.1; 9.21}}. All bursts in α and β frequency ranges are sorted by the time of their occurrence.

The power spectrum $P_J(f)=\left|\hat{Z}_J(f)\right|^2$ of signal $Z_J(t)$ is determined as the squared modulus

of the signal Fourier component $\hat{Z}_J(f)$. This Fourier spectrum is calculated for the entire observation interval of the signal $0 \le t \le 10$ s (Fig.2).

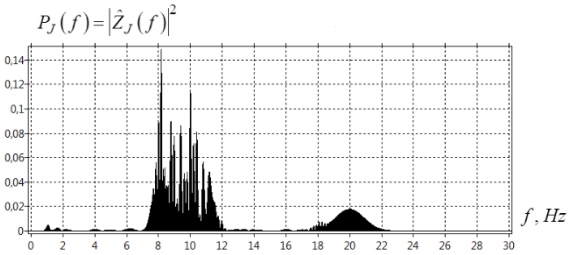

Figure 2: Power spectrum $P_J(f)$ of the signal $Z_J(t)$.

The analysis of the signal power spectrum $P_J(f)$ shows that throughout the signal duration $0 \le t \le 10$ s, its spectrum contains bursts with frequencies in α-range. The chaotic bursts of β-rhythm appear in the range [17-19 Hz]. In addition to these β - bursts, in the power spectrum, we have an ideal Gaussian peak located at $\nu_0 = 20$ Hz with the width $\Delta\nu_0 = 1/\tau_0 \approx 1.1$ Hz. This peak is associated with the model Gaussian burst of activity with the parameters $\{\nu_0; t_0\} = \{20;\ 3.50\}$. Fig.3 represents the modulus $|V_J(\nu,t)|$ of CWT image for signal $Z_J(t)$.

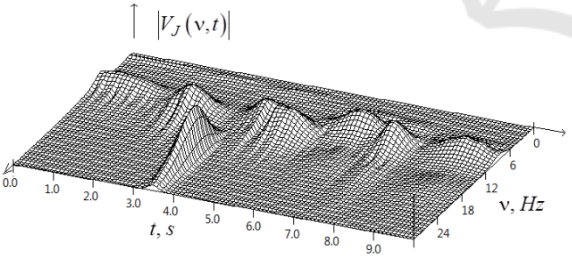

Figure 3: Modulus $|V_J(\nu,t)|$ of CWT image for the signal $Z_J(t)$.

The advantage of applying CWT method over the STFT is that for the CWT method the window size is selected automatically depending on the frequency of the signal. In addition, for the control parameter of the Morlet mother wavelet $m = 1$, the shape of the envelope and the value of the burst frequency completely coincide with the parameters of the test Gaussian signals (Bozhokin et al., 2017).

A similar problem is solved for the second signal $Z_K(t)$ obtained from the central channel $K = C_Z$.

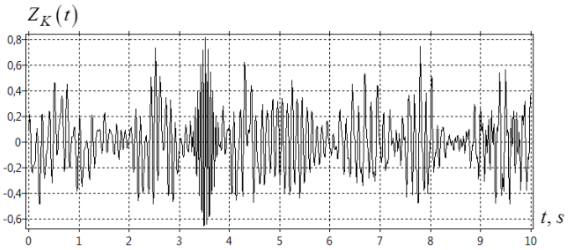

Figure 4: Time dependence of EEG signal $Z_K(t)$ (channel $K = C_Z$).

The matrix of bursts for $Z_K(t)$ in α-range has the form $\alpha MatrixZ_K\{\nu_K; t_K\} = \{\{8.1;\ 0.52\},\ \{12.0;\ 0.52\},\ \{10.1;\ 2.53\},\ \{13.1;\ 2.53\},\ \{8.9;\ 4.31\},\ \{14.0;\ 4.31\},\ \{10.1;\ 5.25\},\ \{8.1;\ 6.68\},\ \{9.0;\ 7.81\},\ \{8.1;\ 9.55\},\ \{6.2;\ 9.27\}\}$. In β-range, the total matrix of bursts in signal $Z_K(t)$ has the form $\beta MatrixZ_K\{\nu_K; t_K\} = \{\{20.0;\ 3.52\}\ \{15.0;\ 5.25\},\ \{16.0;\ 6.73\},\ \{16.9;\ 7.85\},\ \{18.1;\ 9.58\}\}$.

Similarly to signal $Z_J(t)$, we insert an artificial model signal into β-range of the signal $Z_K(t)$ spectrum. It is an ideal Gaussian peak with the characteristics $\{\nu_0; t_1\} = \{20.0;\ 3.52\}$. This specially introduced β-burst in the signal $Z_K(t)$ has the same frequency $\nu_0 = 20$ as that in $Z_J(t)$. However, the burst in the signal $Z_K(t)$ lags behind in time from the burst in the signal $Z_J(t)$ by $\Delta t = t_1 - t_0 = 0.02$ s.

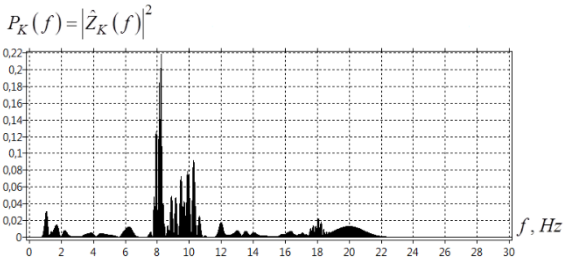

Figure 5: Power spectrum $P_K(f)$ of the signal $Z_K(t)$.

The power spectrum $P_K(f) = |\hat{Z}_K(f)|^2$ for the signal $Z_K(t)$ calculated over the entire observation interval $0 \le t \le 10$ s (Fig.5) differs from that for the

signal $Z_J(t)$ (Fig.2). The power spectrum $P_K(f)$ (Fig.5) has much more bursts in the low-frequency region $f=[1-7$ Hz] δ and θ- rhythms in comparison with the spectrum $P_J(f)$ (Fig.2). The spectrum $P_K(f)$ in α-range [7-14 Hz] has fewer harmonics compared to $P_J(f)$. However, the spectrum of bursts in β-range in the signal $Z_K(t)$ is much wider than in the signal $Z_J(t)$. Fig.6 shows the modulus of CWT $|V_K(\nu,t)|$ for the signal $Z_K(t)$.

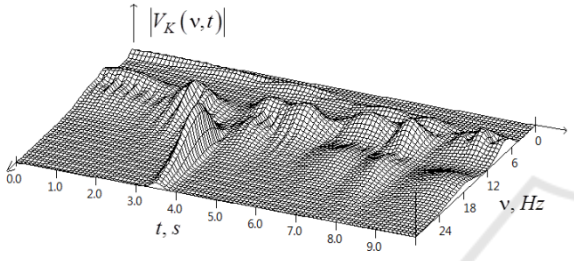

Figure 6: Modulus of CWT $|V_K(\nu,t)|$ for the signal $Z_K(t)$.

Three-dimensional patterns of EEG bursts for the signal $Z_J(t)$ (Fig.3) plotted on the ν, Hz and t, s plane differ from those for $Z_K(t)$ (Fig.6).

To study the dynamics of the rise and fall of the bursts with different frequencies, we introduce spectral integrals $E_\mu(t)$, which depend on time t (Bozhokin and Suvorov, 2008; Bozhokin and Suslova, 2014, 2015).

$$E_\mu(t)=\frac{1}{\Delta\nu}\int_{\nu_\mu-\Delta\nu/2}^{\nu_\mu-\Delta\nu/2}\varepsilon(\nu,t)d\nu\,. \qquad (7)$$

Spectral integral $E_\mu(t)$ is the average value of signal energy spectrum local density $\varepsilon(\nu,t)=2|V(\nu,t)|^2/(\nu C_\psi)$, integrated over the certain frequency interval $[\nu_\mu-\Delta\nu/2;\nu_\mu+\Delta\nu/2]$, where ν_μ is the middle of the corresponding spectral interval, $\Delta\nu$ is the width of the interval. Studying the behavior of spectral integrals over time $E_\mu(t)$, we perform a kind of filtering of our signal by summing the contributions from the local spectrum density $\varepsilon(\nu,t)$ in a certain frequency range $\mu=\{\delta,\theta,\alpha,\beta\}$. The constant C_ψ was calculated in the article (Bozhokin et al, 2017).

To compare the bursts accurately let us consider the values of the spectral integral $E_\alpha(t)$ in the α-range for the signals $Z_J(t)$ and $Z_K(t)$. For this purpose, we take the time interval $t=$ [2-8 s] (Fig.7), where the main bursts of these signals are concentrated.

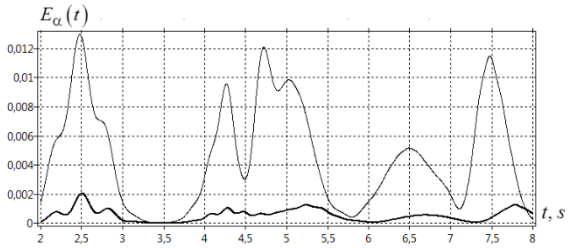

Figure 7: Spectral integrals $E_\alpha(t)$ versus time t for α-range. The thin line corresponds to the signal $Z_J(t)$ (channel O_z). The bold line is for the signal $Z_K(t)$ (channel C_Z).

The analysis of spectral integrals $E_\alpha(t)$ in α-range shows (Fig.7) that the structure of the bursts changes when the disturbance moves from the occipital channel O_Z $(Z_J(t))$ to the channel C_Z $(Z_K(t))$. With this movement, the amplitude of the bursts decreases. The speed $V_\alpha\approx$3-5 m/s of α-burst maximum movement can be estimated from the shift of this maximum, which is $\Delta t\approx$ 0.02-0.03 s.

Thus, using two EEG channels as an example, we have shown that the frequency spectrum and temporal position of bursts change as they propagate through the cerebral cortex. Then, let us calculate the wavelet correlation function $|WCF_{JK}(\nu,t)|$ (5)-(6) for the signals $Z_J(t)$ and $Z_K(t)$. This function will allow us to find the correlation of two bursts, whose maxima of which are located at different time moments for the fixed frequency ν varying in the interval $\nu=[1-30\,Hz]$.

We consider the time argument of $|WCF_{JK}(\nu,t)|$ varying in the interval $t=[-10;10$ s]. The graph of $|WCF_{JK}(\nu,t)|$ is shown in Fig.8.

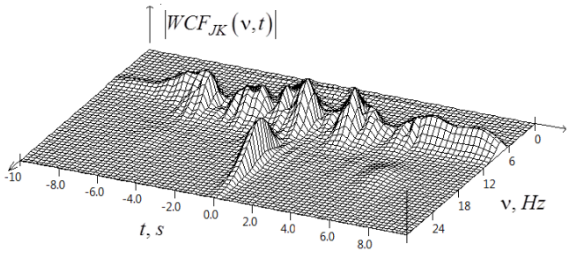

Figure 8: Wavelet correlation function $|WCF_{JK}(\nu,t)|$ of two signals J and K depending on frequency ν, Hz and time t, s.

Let us explain the main peaks of $|WCF_{JK}(\nu,t)|$ in Fig.8. Suppose that there is a single burst in signal $Z_J(t)$, characterized by frequency ν time t_J of its maximum. In this case, the maximum value of CWT image $V_J^*(\nu,t')$ will be observed at the moment of time $t'=t_J$.

In turn, there is a single burst in signal $Z_K(t)$, characterized by the same frequency ν and the time moment t_K. The maximum of $V_K(t+t')$ will be at $t+t'=t_K$. The consequence of these two equalities is the condition that the maximum of $|WCF_{JK}(\nu,t)|$ (5), (6) will be observed at the frequency ν at the moment of time $t=t_K-t_J$.

Let us explain the origin of the maxima in Fig.8 in the range of the alpha rhythm $\alpha=[7;14\,Hz]$ in the time interval $t=[-10;10\,s]$. We introduce the designation $\{\nu_J;t_J\}_J \Leftrightarrow \{\nu_K;t_K\}_K$, which means the correlation of an individual burst $Z_J(t)$, characterized by frequency ν_J and center localization time t_J, with a specific burst having the parameters ν_K and t_K.

The leftmost maximum of $|WCF_{JK}(\nu,t)|$ (Fig.8) is located in the frequency range $\nu=[8;9\ Hz]$ in the time interval $t=[-6;-5\,s]$. This leftmost maximum is associated with the correlations of the following bursts: $\{7.8;6.41\}_J \Leftrightarrow \{8.1;0.52\}_K$; $\{8.8;9.23\}_J \Leftrightarrow \{8.9;4.31\}_K$. The next leftmost maximum of $|WCF_{JK}(\nu,t)|$ is located in the frequency range $\nu=[9;10\ Hz]$ in the time interval $t=[-3.5;-2\,s]$. This maximum is associated with the following correlations: $\{9.8;7.62\}_J \Leftrightarrow \{10.1;5.25\}_K$.

A large number of bursts in α-range, which have approximately the same frequencies and times of occurrence, form a large correlation peak located nearby $t=0$. Reasoning similarly, the rightmost peak of $|WCF_{JK}(\nu,t)|$ located in the interval of times $t=[6-10\,s]$ near the frequencies $\nu\approx 10\,Hz$ is associated with correlations: $\{8.2;0.51\}_J \Leftrightarrow \{8.1;9.55\}_K$; $\{8.2;0.51\}_J \Leftrightarrow \{8.1;6.68\}_K$. The most striking correlation (5), (6) in β-range is a high peak centered at the point $\{20.0;0.02\}$. The reason for this peak is the correlation of two bursts: $\{20.0;3.50\}_J \Leftrightarrow \{20.0;3.52\}_K$.

Thus, we introduced the function $WCF_{JK}(\nu,t)$, which adequately describes the wavelet correlation of two signals $Z_J(t)$ and $Z_K(t)$, each consisting of a large number of EEG bursts. The ensemble of signal bursts $Z_J(t)$ differs from the ensemble of signal bursts $Z_K(t)$ both in the time of their occurrence and in the frequency composition. In addition, each burst has its own amplitude, phase, and characteristic time scale.

4 CONCLUSIONS

The aim of the article is to introduce a new wavelet correlation function $WCF_{JK}(\nu,t)$. The electrical activity of neural ensembles is analyzed using EEG signals from many brain channels in different spectral ranges. We discussed the shortcomings of the methods based on the windowed Fourier transform (short-time Fourier transform - STFT) for the study of the synchronization of various EEG channels. The disadvantages include the ambiguity in the choice of the window duration, the problems of selecting the window function, and the degree of window overlapping.

The known wavelet methods for studying signal correlation make it possible to analyze the interdependence of two EEG signals occurring only at the same time. The study of real EEG signals, in which correlated bursts occur at different times, requires the use of another type of wavelet correlation function.

In the article, we use the modification $V(\nu,t)$ of continuous wavelet transform, which has advantages over the standard CWT form $W(\nu,t)$ (Mallat, 2008; Chui and Jiang, 2013; Hramov, 2015). These involve the accurate reflection of the ratios by both frequencies and amplitudes of the signals and their CWT images. Furthermore, by including an additional control parameter m into the Morlet mother wavelet, we get the opportunity to further adjust both the amplitude and frequency resolution of signals.

An example of two EEG channels is analyzed. The signals from these channels $Z_J(t)$ and $Z_K(t)$ are the alternation of bursts, which occur at different times in different frequency intervals. The spectral powers of these signals $P_J(f)$ and $P_K(f)$ are calculated, as well as their CWT images $V_J(\nu,t)$ and $V_K(\nu,t)$. A new correlation function $WCF_{JK}(\nu,t)$ is introduced and calculated. It allows us to determine the correlation of bursts occurring in signals at different times, but having the same frequency. For the specific example of two nonstationary signals from different EEG channels, a classification of correlations of different bursts is suggested.

The proposed method assuming the calculation of the function $WCF_{JK}(\nu,t)$ can be used to analyze the propagation of disturbances over the surface of the brain, and to study the synchronicity of the evoked potentials arising as a response of neural ensembles to the sensory stimulation. The $WCF_{JK}(\nu,t)$ can be useful in the study of rapidly changing burst processes in plasma physics and astrophysics, as well as for the determination of coherent space-time structures for media with strong dispersion.

ACKNOWLEDGMENTS

The work was performed within the framework of the Russian State tasks for conducting fundamental research (topic code FSEG-2020-0024).

REFERENCES

Addison, P.S., 2017. *The illustrated wavelet transform handbook. Introductory theory and application in Science, engineering, medicine and finance,* CPC Press, Second Edition.

Adeli, H., Ghost-Dastidar, S., 2010. *Automated EEG-based diagnosis of neurological disorders: Inventing the future of neurology,* CRC Press.

Advances in Wavelet Theory and Their Applications in Engineering, Physics and Technology. 2012. Edited by Dumitru Baleanu

Banfi, F., Ferrini, G., 2012. Wavelet cross-correlation and phase analysis of a free cantilever subjected to band excitation, *Beilstein J. Nanotechnol. 3: 294–300.*

Bendat, J. S., and Piersol, A. G., 2011. *Random Data: Analysis and Measurement Procedures, (Vol. 729)*, NY: John Wiley & Sons, New York.

Bozhokin S.V., Suvorov N.B., 2008. Wavelet analysis of transients of an electroencephalogram at photostimulation, *Biomed. Radioelektron, N3: 21-25.*

Bozhokin, S.V., Suslova, I.B., 2014. Wavelet Analysis of Non-Stationary Signals in Medical Cyber-Physical Systems (*MCPS*), International Conference on Next Generation Wire/Wireless Networking, *Lecture Notes of Computer Science, LNCS, 8638: 467-480.*

Bozhokin, S.V., Suslova, I.B., 2015. Wavelet-based analysis of spectral rearrangements of EEG patterns and of non-stationary correlations, *Physica A. 421:151–160.*

Bozhokin, S.V., Zharko, S.V., Larionov, N.V., Litvinov, A.N., Sokolov, I.M., 2017. Wavelet Correlation of Nonstationary Signals, *Technical Physics, 62(6):837-845.*

Chavez, M., Cazelles, B., 2019. Detecting dynamic spatial correlation patterns with generalized wavelet coherence and non-stationary surrogate data, *Scientific Reports 9(1): 7389-7398.*

Chui, C.K., Jiang O., 2013. *Applied Mathematics. Data Compression, Spectral Methods, Fourier Analysis, Wavelets and Applications. Mathematics Textbooks for Science and Engineering*, v.2, Atlantis Press.

Cohen A., 2003. *Numerical Analysis of Wavelet Method,* Elsevier Science, North-Holland.

Duc N.T., Lee B., 2019. Microstate functional connectivity in EEG cognitive tasks revealed by a multivariate Gaussian hidden Markov model with phase locking value, *Journal of neural engineering, 16(2):026033*

Grinsted, A., Moore, J.C., Jevrejeva S., 2004. Application of the cross wavelet transform and wavelet coherence to geophysical time series, *Nonlinear Processes in Geophysics 11(5/6): 561-566.*

Hramov, A.E., Koronovskii, A.A., Makarov, V.A., Pavlov, A.N., Sitnikova, E., 2015. *Wavelets in neuroscience*, Springer Series in Synergetics, Springer-Verlag, Berlin, Heidelberg.

Klein, A., Sauer, T., Jedynak,A., Skrandies,W., 2006. Conventional and wavelet coherence applied to sensory-evoked electrical brain activity, *IEEE transaction on biomedical engineering. 53(2): 266-272.*

Kropotov, J. D., 2010. *Quantitative EEG, Event-Related Potentials and Neurotherapy,* San Diego, CA: Academic Press.

Kulaichev, A.P., 2011. The informativeness of coherence analysis in EEG studies, *Neuroscience and behavioral physiology. 41(3): 321-328.*

Lachaux, J.-P, Lutz, A., Rudrauf, D., Cosmelli, D., Quyen, L.V., Martinerie, J., Varela, F., 2002. Estimating the time-course of coherence between single-trial brain signals: an introduction to wavelet coherence, *Neurophysiologie Clinique. 32: 157-174.*

Li, X., Yau, X., Fox,J., Jefferys,J.G., 2007. Interactions dynamics of neuronal oscillations analysed using wavelet transform, *Journal of Neuroscience Methods. 160:178-185.*

Kang, S.H., McIver,R.P., Hernandes,J.A., 2019. Co-movements between Bitcoin and Gold: A wavelet coherence analysis, *Physica A: Statistical Mechanics and its Applications, 536: 120888.*

Mallat, S., 2008. *A Wavelet Tour of Signal Processing*, Academic Press, New York, 3rd ed.

Mandel L, Wolf E., 1995. *Optical Coherence and Quantum Optics*, Cambridge University Press.

Papandreou-Suppappola A., 2003. *Application in time-frequency signal processing*, CRC Press.

Piqueira J.R.C., 2011. Network of phase-locking oscillators and a possible model for neural synchronization, *Commun. Nonlinear Sci. Numer. Simul., 16(9): 3844–3854*.

Reiser, E. M., Schulter, G., Weiss, E. M., Fink, A., Rominger, C., and Papousek, I., 2012. Decrease of prefrontal-posterior EEG coherence: loose control during social-emotional stimulation, *Brain Cogn.. 80, 144–154.* doi: 10.1016/j.bandc.2012.06.001

Schuck, Jr. A., Bodmann, B.E.J., 2019. On the Development of an Alternative Proposition of Cross Wavelet Analysis for Transient Discrimination Problems, Integral *Methods in Science and Engineering, 409-423.*Springer Nature Switzerland. https://doi.org/10.1007/978-3-030-16077-7

Seleznov I., Zyma I., Kiyono K., Tukaev S., Popov.A., Chernykh M., Shpenkov O., 2019. Detrended fluctuation, coherence, and spectral power analysis of activation rearrangement in EEG dynamics during cognitive workload, *Frontiers in Human Neuroscience*, https://doi.org/10.3389/fnhum.2019.00270

Sheikhani A., Behnam H., 2008. Connectivity analysis of quantitative electroencephalogram background activity in Autism disorders with short time Fourier transform and coherence values, *Congress on Image and Signal Processing. IEEE, DOI: 10.1109/CISP.2008.595*.

Subha, D.P., Joseph, P.K., Acharya, R.U., Lim C.M., 2010. EEG Signal Analysis: A Survey, *Journal of medical systems. 34: 195-212.*

Trofimov, A.G., Kolodkin, I.V., Ushakov, V.L., Velichkovski, B.M., 2015. Agglomerative method for isolating microstates related to the characteristics of the traveling wave, *Neuroinformatic-2015, Russian Scientific and Technical Conference, M.:MIFI. Part 1: 66-77.*

Wavelets in Physics, 2004. Edited by J.C. Van.den Berg, Cambridge University Press.

Yang, Xi. X., Shi C., *et al.,* 2019. Surface Electromyography-Based Daily Activity Recognition Using Wavelet Coherence Coefficient and Support Vector Machine, *Neural Process Lett. 50:2265–2280*.